Histol Histopathol (2008) 23: 781-787
DOI: 10.14670/HH-23.781

http://www.hh.um.es

Histology and Histopathology
Cellular and Molecular Biology

The cellular and subcellular localization of zinc transporter 7 in the mouse spinal cord

Zhi-Hong Chi[1], Hao Ren[1], Xin Wang[1], Ming Rong[1], Liping Huang[2] and Zhan-You Wang[1]

[1]Department of Histology and Embryology, China Medical University, Shenyang, China and [2]Department of Nutrition and Rowe Program in Genetics, USDA/ARS/Western Human Nutrition Research Center, University of California at Davis, Davis, California, USA

Summary. The present work addresses the cellular and subcellular localization of the zinc transporter 7 (ZNT7, SLC30a7) protein and the distribution of zinc ions (Zn^{2+}) in the mouse spinal cord. Our results indicated that the ZNT7 immunoreactive neurons were widely distributed in the Rexed's laminae of the gray matter in all spinal segments examined. The ependyma cells of the central canal and glia cells in the white matter were also shown ZNT7-positive. The ZNT7 immunoreactivity was mainly detected in the perinuclear regions of ZNT7-positive cells in the spinal gray matter. For ependyma cells, the immunoreactivity of ZNT7 was detected in the cytoplasm near the lumina of the central canal. Ultrastructural localization showed that ZNT7 was predominately present in the membrane of the Golgi stacks. The double immunofluorescence studies confirmed this result. Other intracellular organelles including the endoplasmic reticulum, mitochondria and lysosomes were devoid of ZNT7-immunostaining. The chelatable Zn^{2+} ions in the spinal cord were found predominantly in the terminals of the neuron rather than the cell body in the gray matter. However, overlapping distribution of chelatable Zn^{2+} ions and ZNT7 was found in the ependyma cells. The present study supports the notion that ZNT7 may function to supply zinc ions to the newly synthesized metalloproteins in the secretory pathway of the spinal neuron and the ependyma cell.

Key words: Zinc, Zinc transporter, Golgi apparatus, Spinal cord, Zinc selenide autometallography

Offprint requests to: Zhan-You Wang MD, PhD, Department of Histology and Embryology, China Medical University, Shenyang 110001, P.R. China. e-mail: wangzy@mail.cmu.edu.cn

Introduction

In the mammalian central nervous system (CNS), many regions contain large amount of Zn^{2+}, such as hippocampus, olfactory bulb, amygdala cortex, and spinal cord (Schroder, 1977; Takeda, 2001). In mammals, zinc transport across the membrane is mediated by two zinc transporter families, ZIP (ZRT, IRT-like protein, SLC39) and ZNT (zinc transporter, SLC30) (Kambe et al., 2004). The ZIP family members are involved in zinc influx into the cytosol from the extracellular space and the lumen of intracellular organelles, while the ZNT family members have opposite roles in cellular zinc homeostasis (Colvin et al., 2003; Kambe et al., 2004). ZNTs, except ZNT5, are predicted to have six transmembrane domains and a large histidine-rich intracellular loop between domains 4 and 5 which is proposed to be the zinc binding site. To date, eight *Znt* genes, named *Znt1* to *Znt8*, have been cloned and characterized (Seve et al., 2004). Two other *Znt* genes (*Znt9* and *Znt10*) were predicted by the mouse and human genome resources (Sim and Chow, 1999; Seve et al., 2004). Among the ZNT proteins, ZNT1 is the only transporter that is responsible for transporting zinc from the cytosol to the extracellular space. The others (ZNT2-8) are involved in pumping zinc into different intracellular organelles when the cellular zinc level is elevated (Kambe et al., 2004).

The spinal cord contains a large amount of Zn^{2+} (Danscher et al., 2001; Wang et al., 2001a), but little is known about zinc metabolism in the spinal cord. Zinc autometallographic (AMG) studies have shown that free zinc ions are dispersed throughout the gray matter (Schroder, 1977; Schroder et al., 1978; Jo et al., 2000). At electron microscopic levels, free zinc ions were found in terminals of subgroups of GABAergic, glycinergic

and glutamatergic neurons in the spinal cord (Martinez-Guijarro et al., 1991; Beaulieu et al., 1992; Wang et al., 2001b). The findings of zinc-containing terminals presynaptic to neuronal somata and dendrites of dorsal and ventral horns suggest that zinc may be involved in both sensory transmission and motor control at the spinal cord level (Jo et al., 2000).

We have recently reported that five members of the zinc transporter family, ZNT1, ZNT3, ZNT4, ZNT6 and ZNT7 are abundantly expressed in mouse and rat brains (Wang et al., 2004; Chi et al., 2006). In the spinal cord, however, only the distribution of ZNT3 has been characterized in detail (Jo et al., 2000; Danscher et al., 2003). ZNT7 was identified by searching the expressed sequence tag (EST) databases with the amino acid sequence of ZNT1 (Kirschke and Huang, 2002). It is localized in the Golgi apparatus of mouse choroid epithelial cells demonstrated by our electron microscopic study (Chi et al., 2006). Zinc exposure to the ZNT7-overexpressing Chinese hamster ovary (CHO) cells caused an accumulation of zinc in the Golgi apparatus, suggesting that ZNT7 facilitates zinc transport from the cytosol into the Golgi complex (Kirschke and Huang, 2002). The goal of the present study is to investigate the cellular and subcellular distribution of ZNT7 in the mouse spinal cord.

Materials and methods

Mice

Eight male CD-1 mice (8-10 weeks old, 30-35g, provided by the experimental animal center of China Medical University) were used in the present study. They were housed under a 12h light/dark cycle, with water and food available *ad libitum*. All procedures were carried out in accordance with the ethical standards of China Medical University.

Immunohistochemistry

Four mice were deeply anesthetized with sodium pentobarbital (50 mg/kg, i.p.), and were perfused transcardially with isotonic saline, followed by 4% paraformaldehyde in 0.1M phosphate buffer (PB, pH 7.4) for light immunohistochemistry and immunofluorescence labeling, or 4% paraformaldehyde and 0.025% glutaraldehyde in 0.1 M PB for electron microscopy. The entire spinal cords were carefully removed and cut in 5- to 7-mm thick transverse slabs, which were further post-fixed by immersion into the corresponding fixatives for 3h at 4°C.

For light microscopy, the fixed segments of spinal cord were immersed in a 30% sucrose solution made in PB for overnight at 4°C. Subsequently, segments of spinal cord were cut in 10-μm sections on a freezing microtome (JUNG CM 1800, Leica, Germany) and mounted on glass slides. The sections were rinsed twice in Tris-buffered saline (TBS, pH 7.4), and treated with 3% hydrogen peroxide (H_2O_2) in PB for 10 min to reduce endogenous peroxidase activity. After rinsing with TBS, all tissue sections were preincubated for 1h with 5% bovine serum albumin (BSA) and 3% goat serum in TBS to reduce nonspecific staining. Afterward, the sections were incubated with anti-ZNT7 serum (an affinity-purified rabbit antibody specific for ZNT7) (Kirschke and Huang, 2002), diluted 1:100 in TBS containing 3% goat serum and 1% BSA and 0.3% Triton-X 100 overnight at 4°C. After extensive washing in TBS, sections were incubated with a 1:200 diluted biotinylated anti-rabbit IgG for 1 h at room temperature (RT). The ABC Kit was then applied for 1 h at RT in order to visualize the reaction sites. The ABC solution was diluted 1:100 in TBS. A brown color appeared in the sections after incubation of the sections in 0.025% 3,3'-diaminobenzidine with 0.0033% H_2O_2 for 10 min at RT. The sections were dehydrated in graded alcohols and coverslipped with neutral balsam for light microscopy.

For electron microscopy, transversal sections were cut at 50 μm on a vibratome and collected in 0.1 M PB at RT. Immunostaining was performed on free floating vibratome slices. The sections were incubated with an affinity-purified anti-ZNT7 antibody diluted 1:50 in TBS containing 1% BSA and 0.25% dimethylsulfoxide overnight at 4°C. Subsequently, the tissue sections were processed by using the ABC procedure and DAB/hydrogen peroxide as above. Sections were eventually osmicated for 30min in 1% osmium tetroxide (OsO_4) made in 0.1 M PB at RT. After alcohol dehydration and propylene substitution, sections were flat-embedded in Epon 812. Semithin sections were prepared with an ultramicrotome and stained with 0.1% toluidine blue for light microscopic examinations. Ultrathin sections were collected on mesh nickel grids, stained with uranyl acetate for 10 min, and examined at 80 kV in an electron microscope (JEM-1200EX).

For confocal immunofluorescence microscopy, samples were rinsed in PB and placed in 30% sucrose until they sank to the bottom of the container. After rinsing, samples were cut into 10 μm sections in a cryostat and mounted on glass slides. Subsequently, sections were preincubated with normal donkey serum (1:20) for 1 h, then incubated overnight at RT with anti-ZNT7 serum at 1:100, and anti-TGN38 (monoclonal antibody, Sigma) at 1:100. Secondary antibodies used were fluorescein isothiocyanate (FITC)-conjugated donkey anti-rabbit (FITC-DAR) IgG, and Texas Red-conjugated donkey anti-mouse (Texas Red-DAM) IgG purchased from Jackson ImmunoResearch. After rinsing with PBS, the sections were incubated for 2 h with DAR-FITC (1:50) and Texas Red-DAM (1:50) at RT. Then the sections were mounted and examined in a confocal laser scanning microscope (CLSM, SP2, Leica, Germany).

To assess nonspecific staining, a few sections in every experiment were incubated with normal sera instead of ZNT7 primary antibody. This procedure always resulted in a complete lack of immunoreactivity.

Zinc selenide autometallography (ZnSe^{AMG})

Four mice were injected i.p. with sodium selenide dissolved in 0.1 M PB (25 mg/kg). After 1.5 h survival time, the animals were then deeply anesthetized and transcardially perfused with a 2.5% glutaraldehyde solution in 0.1 M PB. Tissue isolation and fixation were performed as described above. After post-fixing for 3 h, samples were cut in 10 μm coronal sections on a cryostat and placed on glass slides pre-treated with Farmer solution to avoid contamination. Sections were then incubated in the AMG developer in a water bath for 1h at 26°C as described by our previous study (Danscher, 1982). Subsequently, sections were immersed in a 5% thiosulphate solution to stop the AMG reaction, followed by placing under running tap water for 20 min in order to remove the gelatine membrane. The sections were then dehydrated and coverslipped with neutral balsam for light microscopy.

Results

Light microscopy of immunohistochemistry and ZnSe^{AMG}

The ZNT7 immunoreactivity and ZnSe^{AMG} staining patterns were very different to each other in both the dorsal and ventral horns of the spinal cord (Fig. 1). The ZNT7 immunoreactivity appeared to be located in the neuronal cell body and there was no visible distinction in the intensity of immunolabeling and staining patterns in different laminae (Fig. 1a). ZnSe^{AMG} staining was found predominantly in the terminals of the neuron and caused a characteristic segmental laminar pattern (Fig. 1b), indicating that there is no correlation between ZNT7 immunostaining and ZnSe^{AMG} stating in the neuronal cell body. In the dorsal horn, the ZnSeAMG staining was more intensive in the superficial laminae (I, III-IV) than in the deeper laminae (V-VI). In the ventral horn, the staining was observed in the large terminals. Laminae VII and X were densely stained at all segmental levels with variably sized zinc-enriched terminals (Fig. 1b). It is notable that the ZNT7 immunohistochemistry and ZnSe^{AMG} staining patterns were pronounced and corresponded to each other in ependyma cells of the central canal of the spinal cord. Both staining products were localized in the cytoplasm near to the central canal (Fig. 2a,b).

Fig. 3 shows the overall immunocytochemical staining of ZNT7 in the mouse spinal cord. In the gray matter (Fig. 3a-d), ZNT7-positive neurons were widely distributed in all laminae including interneurons of Rexed's laminae I-IV and the motor neurons of laminae

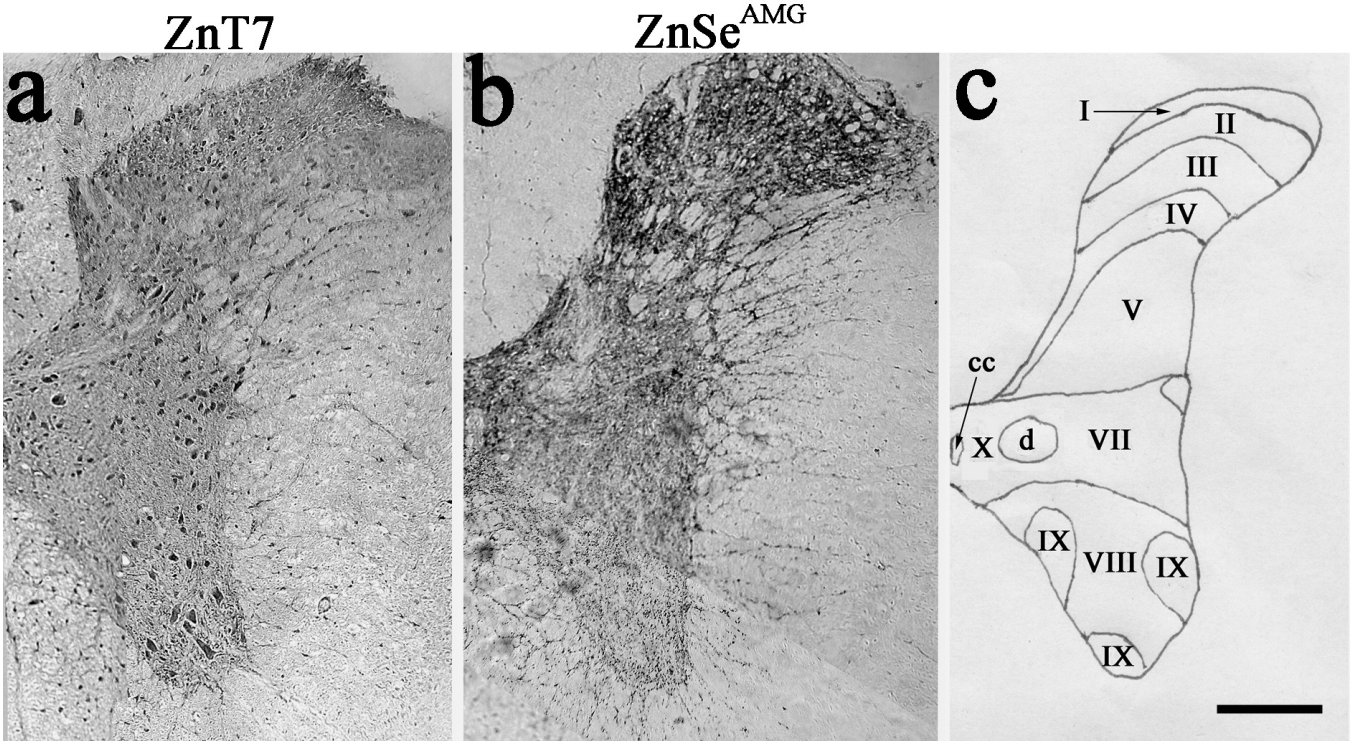

Fig. 1. Light photomicrographs from the upper thoracic segment of mouse spinal cord taken from transverse 10 μm cryosections stained by ZNT7 immunohistochemistry **(a)** and ZnSe^{AMG} **(b)**. Note the relation of the staining pattern to the Rexed's laminae **(c)**. ZNT7 immunoreactivity was located in the neuronal cell body and there was no visible distinction between the intensity of immunolabeling and staining patterns in different laminae. ZnSeAMG staining was located in the terminals of the neuron and appeared to be a characteristic segmental laminar pattern. Scale bar: 200 μm.

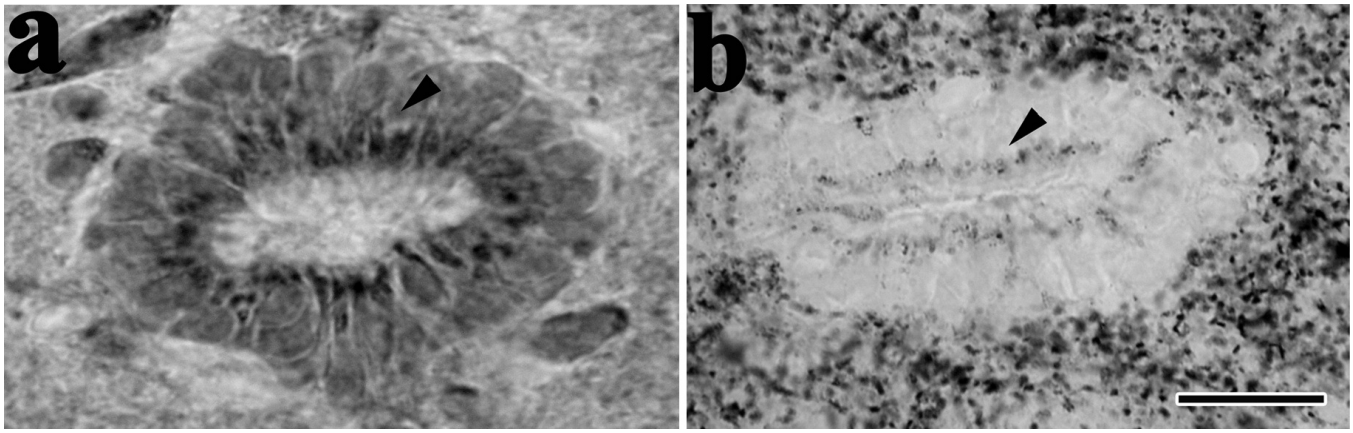

Fig. 2. Distribution of the ZNT7-immunoreactivity and ZnSeAMG staining in the ependyma cells of the mouse spinal cord. Both ZNT7 immunoreactivity **(a)** and $ZnSe^{AMG}$ **(b)** staining were located in the cytoplasm near the lumina of the central canal. Scale bar: 20 μm.

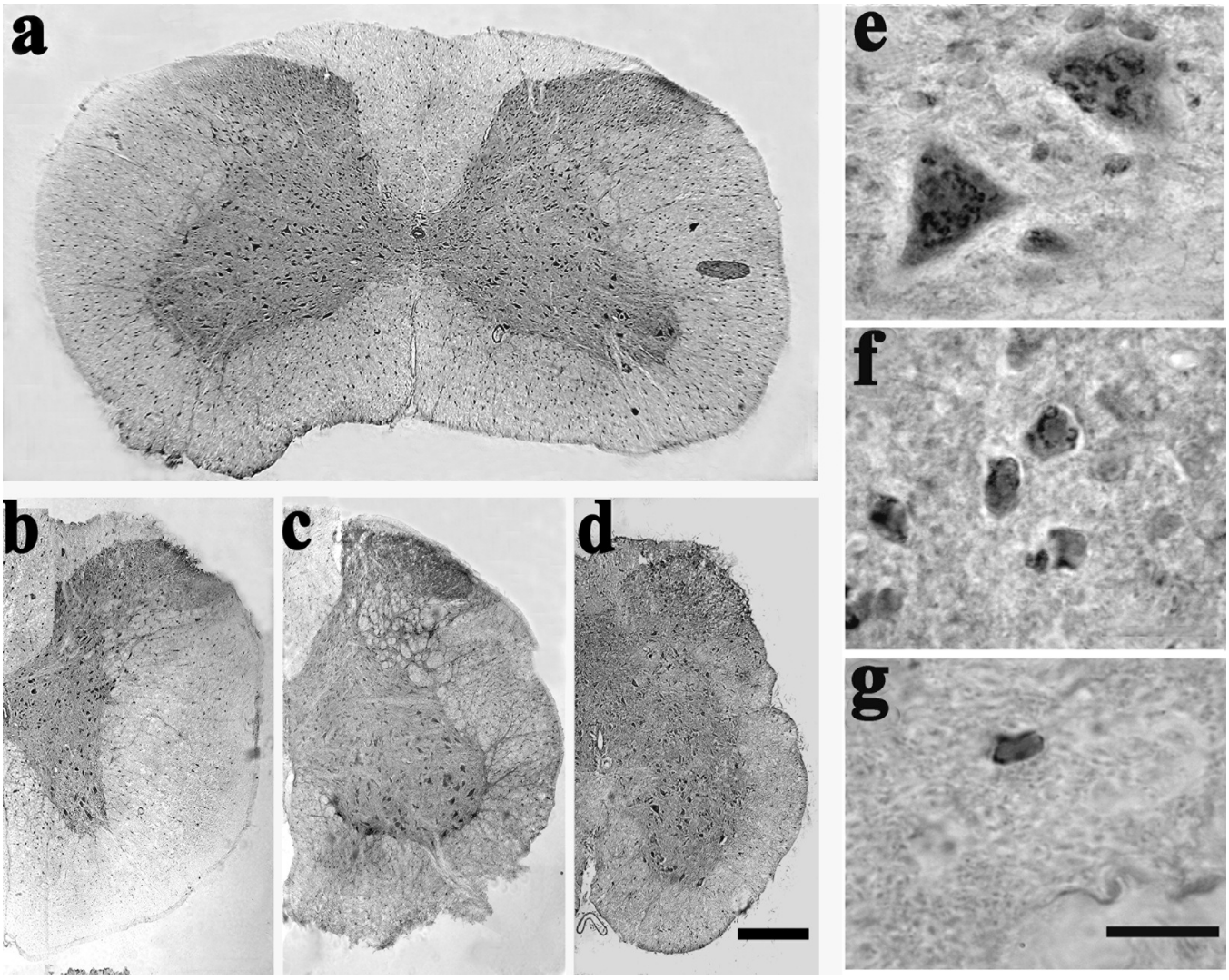

Fig. 3. Light photomicrographs of transverse 10 μm cryosections stained with an anit-ZNT7 antibody on the cervical **(a)**, upper thoracic **(b)**, upper lumbar **(c)**, and upper sacral **(d)** spinal segments. ZNT7-immunoreactive cells were widely distributed in the gray matter including interneurons of laminae I-IV and motor neurons of laminae VIII-IX. There were no visible difference in the intensity of immunolabeling and staining patterns among the different segments. The higher magnification pictures showed that the ZNT7 immunostaining was predominantly located in the perinuclear region of the motor neurons **(e)**, interneurons **(f)**, and glia cells **(g)**. Scale bars: a-d, 200 μm; e-g, 20 μm.

VIII-IX. The ZNT7 immunolabeled neurons differed in shape and size. In the white matter, glia cells were positive for ZNT7 immunoreactivity. At a higher magnification, the immunoreactivity of ZNT7 was concentrated in the perinuclear regions of the neuronal cell body (Fig. 3e-g), suggesting a Golgi apparatus localization of ZNT7.

Ultrastructural localization of ZNT7

Electron microscopic immunolocalization confirmed the presence of ZNT7 in the Golgi apparatus of neurons. At the ultrastructural level where the Golgi apparatus was clearly detectable and localized in the perinuclear region, and ZNT7 immunoreactivity was found in all elements of the Golgi stacks including the cis- and trans-face (Fig. 4). In addition, the Golgi vesicles were positive for the ZNT7 immunoreactivity. On the other hand, transport vesicle buds from the endoplasmic reticulum (ER) were devoid of the ZNT7 immunostaining. As expected, the ZNT7 immunoreactivity appeared to be located on the membrane rather than in the lumen of the Golgi cisternae. In no case was the ZNT7-immunoreactivity found in other neuronal organelles including rough endoplasmic reticulum, mitochondria, and lysosomes.

Dual immunofluorescence of ZNT7 and TGN38

To further test the above result that ZNT7 is located in Golgi apparatus of neurons of mouse spinal cord, double labeling of ZNT7 and TGN38 was performed to analyze the subcellular localization of ZNT7 in the spinal neurons. Under CLSM, the number of ZNT7-positive neurons and TGN38-positive neurons were adqulis at low magnification (Fig. 5a1, a2, b1, b2). Dual immunofluorescence localization of ZNT7 and TGN38 indicated abundant labeling of both antigens in both the dorsal and ventral horns of the spinal cord, and both labeling was predominantly in the neuronal cell bodies. At high magnification, the filaceous distribution of ZNT7 and TGN38 immunoreactivty was concentrated in the perinuclear regions of both motorneuron in the ventral horn and interneuron in the dorsal horn (Fig. 5c1, c2, d1, d2). The patterns of ZNT7 and TGN38 immunoreactivity were almost completely identical. After merging the ZNT7- and TGN38-labeled images from the two channels, a colocalization of ZNT7 and TGN38 could be demonstrated (Fig. 5a3, b3, c3, d3).

Discussion

The functional significance of zinc in the spinal cord is not very well understood. Our previous retrograde tracing study has demonstrated that zinc-containing neuronal somata appears in most regions of laminae III to X in the spinal cord (Wang et al., 2001a). Neuronal terminals that contain both free zinc ions and the ZNT3 protein were found throughout the mouse spinal cord (Jo et al., 2000; Danscher et al., 2001). It has been confirmed that ZNT3 is localized on the membrane of presynaptic vesicles and serves to sequester the cytoplasmic zinc into synaptic vesicles (Wenzel et al., 1997). As a neuromodulator, the vesicular zinc is released into the synaptic cleft during synaptic activities and interacts with amino acid receptors on the synaptic plasma membrane (Wenzel et al., 1997). In the present study, we report that the expression of the ZNT7 protein is widespread throughout the mouse spinal cord. We also provide data on the subcellular localization of ZNT7 in neurons of the mouse spinal cord.

We previously reported that ZNT7 is localized at the Golgi apparatus and the Golgi vesicles of mouse choroid epithelial cells (Chi et al., 2006). In the present study, our electron microscopic and double immunofluorescence studies demonstrated that, in the neurons of the mouse spinal cord, ZNT7 displayed a similar distribution pattern. From the functional point of view, the Golgi complex plays important roles in modification, packing, sorting, and dispatching proteins into appropriate cellular compartments. It is well known that numerous proteins are properly folded by binding to zinc ions during their itinerary in the biosynthetic-secretory

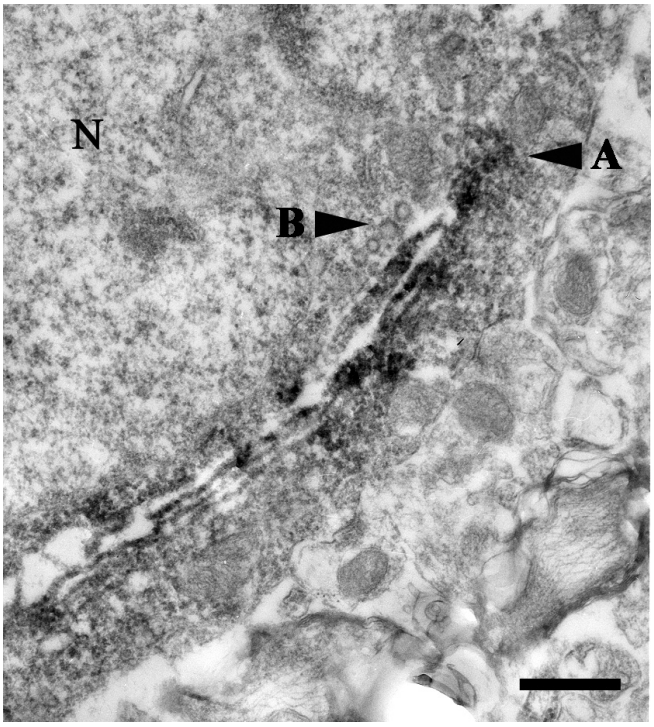

Fig. 4. Electron micrograph showing ZNT7 immunoreactivity in the motor neuron of the mouse spinal cord. The ZNT7-immunoreactivity is predominantly located in all elements of the Golgi stacks. The Golgi vesicles were also ZNT7 positive (arrowhead A), but the trans cisterna of the Golgi complex and the transport vesicles bud from the ER appeared to be devoid of the ZNT7 immunostaining (arrowhead B). Scale bar: 500 nm.

pathway. Therefore, it is reasonable to assume that ZNT7 may be involved in protein modifications and packing in the Golgi apparatus by transporting the cytoplasmic zinc into the lumen of the Golgi complex in neuronal cells of the mouse spinal cord.

We previously reported that the distribution of free zinc ions and ZNT7 in the mouse choroid plexus and retina overlaps (Chi et al., 2006; Wang et al., 2006). However, in the mouse spinal cord, the overlapped staining for both free zinc ions and ZNT7 was only observed in ependyma cells. In the neuronal cells of the spinal cord, free Zn^{2+} ions appear predominantly in the terminals of the neurons rather than the cell body where ZNT7 is localized. Other members of the ZNT family, such as ZNT5 and ZNT6, are also localized in the Golgi apparatus in many tissues (Huang et al., 2002; Inoue et al., 2002; Kambe et al., 2002; Suzuki et al., 2005). Therefore, ZNT7 may not be the only transporter to pump zinc from the cytosol into the Golgi apparatus. As the result, it becomes necessary to identify different roles for these zinc transporters in transporting zinc into the Golgi apparatus in the future.

Glia cells are believed to be involved in zinc metabolism due to their abundant expression of metallothioneins (El Refaey et al., 1997). In the mouse cerebellum, the Bergman glia cells show strong immunoreactivities of ZNT1, ZNT3, ZNT4 and ZNT6 (Wang et al., 2005). In the present study, we demonstrated that glia cells in the spinal white matter exhibited the ZNT7 immunoreactivity. Taken together, these findings support the notion that glia cells are very important for maintaining zinc homeostasis in the CNS.

In conclusion, immunocytochemistry of ZNT7 demonstrated a wide distribution of ZNT7 in the spinal neurons and glia cells located in the gray and white matter, respectively. Electron microscopic immunolocalization confirmed the presence of ZNT7 on the membranes of the Golgi apparatus in neurons located in the dorsal and ventral horns. The abundant presence of ZNT7 in the Golgi apparatus and the similar distribution of ZNT7 and Zn^{2+} in the ependyma cells indicate that ZNT7 may play an important role in delivery of the cytoplasmic zinc to the secretory pathway for the modification and packing of zinc-binding proteins in the

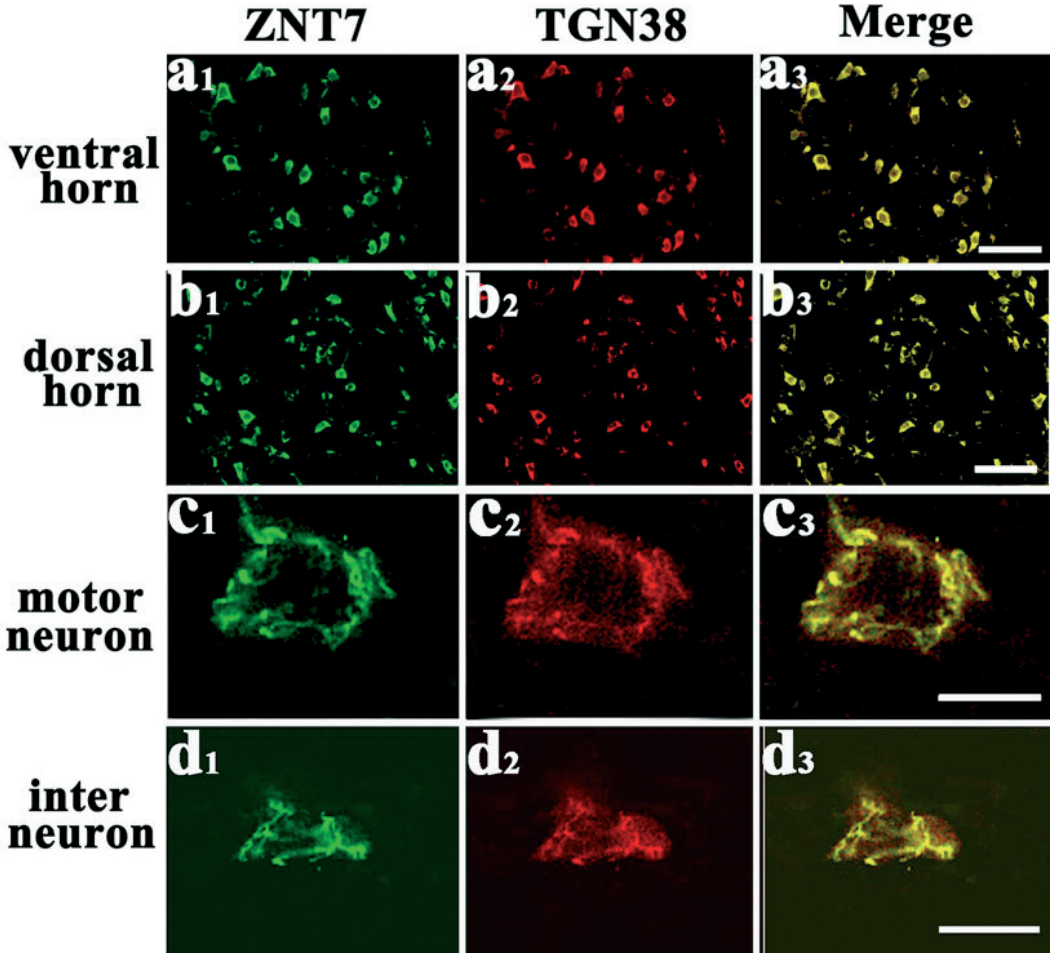

Fig. 5. Colocalization of ZNT7 and TGN38 in the mouse spinal neurons. Confocal images were collected from the spinal ventral **(a1-a3)** and dorsal horn **(b1-b3)** of cryosections double-labelled with ZNT7 **(a1, b1)** and TGN38 **(a2, b2)**, respectively. Scale bars: 75 μm. Both ZNT7 and TGN38 immunoreactivities were found predominantly in the perinuclear Golgi region of the spinal neuronal cell bodies. Colocalization of ZNT7 and TGN38 suggested a Golgi apparatus localization of ZNT7 in the ventral motor neuron **(c1-c3)**, and the dorsal interneuron **(d1-d3)**. Scale bars: 20 μm.

mouse spinal cord.

Acknowledgements. Supported by Natural Science Foundation of China (NSFC-30670722, NSFC-30370452), Specialized Research Fund for the Doctoral Program of Higher Education (SRFDP-20060159001), Program for New Century Excellent Talents in University (NCET-04-0288), China Postdoctoral Science Foundation (2005037008), and the United States Department of Agriculture (CRIS-5603-515-30-014-00D).

References

Beaulieu C., Dyck R. and Cynader M. (1992). Enrichment of glutamate in zinc-containing terminals of the cat visual cortex. NeuroReport 3, 861-864.

Chi Z.H., Wang X., Wang Z.Y., Gao H.L., Dahlstrom A. and Huang L. (2006). Zinc transporter 7 is located in the cis-Golgi apparatus of mouse choroid epithelial cells. Neuroreport 17, 1807-1811.

Colvin R.A., Fontaine C.P., Laskowski M. and Thomas D. (2003). Zn^{2+} transporters and Zn2+ homeostasis in neurons. Eur. J. Pharmacol. 479, 171-185.

Danscher G. (1982). Exogenous selenium in the brain. A histochemical technique for light and electron microscopical localization of catalytic selenium bonds. Histochemistry 76, 281-293.

Danscher G., Jo S.M., Varea E., Wang Z.Y., Cole T.B. and Schroder H.D. (2001). Inhibitory zinc-enriched terminals in mouse spinal cord. Neuroscience 105, 941-947.

Danscher G., Wang Z.Y., Kim Y.K., Kim S.J. and Sun Y. (2003). Immunocytochemical localization of zinc transporter 3 in the ependyma of the mouse spinal cord. Neurosci. Lett. 342, 81-84.

El Refaey H., Ebadi M., Kuszynski C.A., Sweeney J. and Hamada F.M. (1997). Identification of metallothionein receptors in human astrocytes. Neurosci. Lett. 231, 131-134.

Huang L., Kirschke C.P. and Gitschier J. (2002). Functional characterization of a novel mammalian zinc transporter, ZnT6. J. Biol. Chem. 277, 26389-26395.

Inoue K., Matsuda K., Itoh M., Kawaguchi H., Tomoike H. and Aoyagi T. (2002). Osteopenia and male-specific sudden cardiac death in mice lacking a zinc transporter gene, Znt5. Hum. Mol. Genet. 11, 1775-1784.

Jo S.M., Danscher G., Schroder H.D., Won M.H. and Cole T.B. (2000). Zinc-enriched (ZEN) terminals in mouse spinal cord: immunohistochemistry and autometallography. Brain Res. 870, 163-169.

Kambe T., Narita H., Yamaguchi-Iwai Y., Hirose J. and Amano T. (2002). Cloning and characterization of a novel mammalian zinc transporter, zinc transporter 5, abundantly expressed in pancreatic beta cells. J. Biol. Chem. 277, 19049-19055.

Kambe T., Yamaguchi-Iwai Y., Sasakib R. and Nagao M. (2004). Overview of mammalian zinc transporters. Cell. Mol. Life Sci. 61, 49-68.

Kirschke C.P. and Huang L. (2002). ZnT7, a novel mammalian zinc transporter, accumulates zinc in the Golgi apparatus. Cell. Mol. Life Sci. 278, 4096-4102.

Martinez-Guijarro F.J., Soriano E., Del Rio J.A. and Lopez-Garcia C. (1991). Zinc-positive boutons in the cerebral cortex of lizards show glutamate immunoreactivity. J. Neurocytol. 20, 834-843.

Schroder H.D. (1977). Sulfide silver architectonics of rat, cat, and guinea pig spinal cord. A light microscopic study with Timm's method for demonstration of heavy metals. Anat. Embryol. 150, 251-267.

Schroder H.D., Fjerdingstad E., Danscher G. and Fjerdingstad E.J. (1978). Heavy metals in the spinal cord of normal rats and of animals treated with chelating agents: a quantitative (zinc, copper, and lead) and histochemical study. Histochemistry 56, 1-12.

Seve M., Chimienti F., Devergnas S. and Favier A. (2004). In silico identification and expression of SLC30 family genes: an expressed sequence tag data mining strategy for the characterization of zinc transporters' tissue expression. BMC Genomics 5, 32.

Sim D.L. and Chow V.T. (1999). The novel human HUEL (C4orf1) gene maps to chromosome 4p12-p13 and encodes a nuclear protein containing the nuclear receptor interaction motif. Genomics 59, 224-233.

Suzuki T., Ishihara K., Migaki H., Matsuura W. and Kohda A. (2005). Zinc transporters, ZnT5 and ZnT7, are required for the activation of alkaline phosphatases, zinc-requiring enzymes that are glycosylphosphatidylinositol-anchored to the cytoplasmic membrane. J. Biol. Chem. 280, 637-643.

Takeda A. (2001). Zinc homeostasis and functions of zinc in the brain. Biometals 14, 343-351.

Wang X., Wang Z.Y., Gao H.L., Danscher G. and Huang L. (2006). Localization of ZnT7 and zinc ions in mouse retina-immunohistochemistry and selenium autometallography. Brain Res. Bull. 71, 91-96.

Wang Z.Y., Danscher G., Mook Jo S., Shi Y., Daa Schroder H. (2001a). Retrograde tracing of zinc-enriched (ZEN) neuronal somata in rat spinal cord. Brain Res. 900, 80-87.

Wang Z.Y., Li J.Y., Dahlström A. and Danscher G. (2001b). Zinc-enriched GABAergic terminals in mouse spinal cord. Brain Res. 921, 165-172.

Wang Z.Y., Stoltenberg M., Huang L., Danscher G. and Dahlström A. (2005). Abundant expression of zinc transporters in Bergman glia of mouse cerebellum. Brain Res Bull. 64, 441-448.

Wang Z.Y., Stoltenberg M., Jo S.M., Huang L., Larsen A., Dahlström A. and Danscher G. (2004). Dynamic zinc pools in mouse choroid plexus. Neuroreport 15, 1801-1804.

Wenzel H.J., Cole T.B., Born D.E., Schwartzkroin P.A. and Palmiter R.D. (1997). Ultrastructural localization of zinc transporter-3 (ZnT-3) to synaptic vesicle membranes within mossy fiber boutons in the hippocampus of mouse and monkey. Proc. Natl. Acad. Sci. USA 94, 12676-12681.

Accepted December 7, 2007